JOURNAL OF CATALYSIS **172,** 211–221 (1997)
ARTICLE NO. CA971851

Physicochemical Characterisation and Catalytic Activity of Primary Amine Templated Aluminosilicate Mesoporous Catalysts

Robert Mokaya[1] and William Jones

Department of Chemistry, University of Cambridge, Lensfield Road, Cambridge CB2 1EW, United Kingdom

Received May 23, 1997; revised July 15, 1997; accepted July 22, 1997

Primary amines are used as structure-directing agents in the room temperature assembly of aluminosilicate inorganic species to yield mesoporous materials with physical and textural properties similar to those of MCM-41 but with substantially higher Brønsted acidity. Si and Al are incorporated into the mesoporous framework in proportions dependent on the gel Si/Al ratio. Calcination of the as-synthesised material to remove the occluded amine generates Brønsted acid sites which (depending on Si/Al ratio) are stronger or comparable in strength to those on zeolite-HY (Si/Al = 3.65) but weaker than those on ultrastable-Y zeolite (USY). The materials, designated Al-MMS, exhibit higher Brønsted acidity and catalytic activity for the cracking of cumene compared to equivalent aluminosilicate MCM-41 materials or to amorphous silica-alumina and show considerable stability to catalytic deactivation. Al-MMS samples with Si/Al ratio $\leq$20 have catalytic activity higher than the zeolite-HY but exhibit a lower rate of deactivation compared to the zeolite. Ageing of the materials (for 1 year in the calcined form) has no significant effect on their acidity and catalytic activity. Hexagonal ordering and total Brønsted acidity (but not acid strength) of the Al-MMS materials may be improved by using prepolymerised aluminosilicate inorganic precursors. © 1997 Academic Press

INTRODUCTION

One of the main goals of research in catalysis over the past decade has been to design catalysts that carry over the crystallinity and well-defined structure of zeolites into the mesoporous range. The recent synthesis of the M41S family of siliceous solids with sharply distributed pores of diameter in the 20–100 Å range has therefore to some extent achieved this goal (1–3). Of particular interest are MCM-41 type materials which, although lacking strict crystallographic order on the atomic level, possess a hexagonal array of uniform pores. To be catalytically active such silica molecular sieves have to be modified by framework substitution to create active sites. Modification may be achieved by incorporation of heteroatoms into the otherwise electrically neutral siliceous framework. For example Brønsted acid sites may be generated in MCM-41 by isomorphous substitution of Al for Si during hydrothermal synthesis. During synthesis quaternary ammonium micelles act as templates for the self assembly of charged aluminosilicate inorganic precursor. This is followed by ammonium exchange of the (calcined) template free material and further calcination to generate protons (4–6). We have recently reported preliminary findings on the synthesis, acidity and catalytic properties of protonic aluminosilicate mesoporous molecular sieve (Al-MMS) materials prepared using primary amines as the templates (7, 8). In our synthetic approach the primary amine surfactants act as structure directing agents (during the self assembly of soluble silicon/aluminium species) and also as a source of charge balancing protons (during calcination of the as-synthesised material). As a result the need for an ammonium exchange and further calcination step which is known to result in the undesirable loss of framework Al is avoided. We note that the need for ammonium exchange does not always arise from the choice of surfactant; H-MCM-41 can be obtained with quaternary ammonium surfactants without further ion exchange if a Na free synthetic gel is used.

Here we report, in detail, the properties of Al-MMS catalysts with bulk Si/Al ratio between 5 and 40 prepared at room temperature using dodecylamine as template. Tetraethyl orthosilicate (TEOS) and aluminium isopropoxide ($Al(OPr^i)_3$) were used as the source of silica and alumina, respectively. We show that Si and Al are incorporated into the mesoporous framework in proportions dependent on the synthetic gel Si/Al ratio. Our findings indicate that whilst the structural properties of Al-MMS materials are similar to those of aluminosilicate MCM-41, the former possess significantly higher Brønsted acidity and are consequently more active for the cracking of cumene. The number of Brønsted acid sites generated in the Al-MMS materials is dependent on the Si/Al ratio. The Si/Al ratio also affects the proportion of strong acid sites but has no effect on the strength of the strongest acid sites. The catalytic activity (for the cracking of cumene) of Al-MMS materials is found to be higher than that of equivalent MCM-41 and amorphous silica-alumina; comparable

[1] E-mail: rm140@cus.cam.ac.uk.

0021-9517/97 $25.00

or higher (depending on Si/Al ratio) than that of zeolite-HY (Si/Al = 3.65); but lower than that of ultrastable-Y zeolite (USY). We also report on the stability of the Al-MMS catalysts and show that they are stable both to catalytic deactivation and ageing. We also show that adding polymerised Al–O–Si species (obtained by heating a mixture of TEOS/Al(OPr^i)$_3$ at 70°C for 4 h) to the amine yields better ordered Al-MMS catalysts with higher acidity and catalytic activity, compared to catalysts obtained when a physical mixture of TEOS/Al(OPr^i)$_3$ (which presumably contains discrete Si and Al species) is added to the amine. This procedure does not, however, affect the strength of the strongest acid sites generated.

METHODS

Materials

The aluminosilicate materials (Al-MMSX, where X is the Si/Al ratio used in the synthesis gel) were prepared using two methods; (i) mixtures of aluminium isopropoxide (Al(OPr^i)$_3$ in 35 ml isopropyl alcohol) and 0.2 mol tetraethylorthosilicate (TEOS, in 80 ml ethanol) at (Si/Al) molar ratios in the range 40 : 1–5 : 1 were heated with vigorous stirring at 70°C for 4 h before adding to 0.05 mol dodecylamine (in a mixture of 80 ml water and 120 ml ethanol at room temperature); (ii) As (i) above, except that the TEOS/Al(OPr^i)$_3$ mixture was added directly to the template solution without heating. The pH of the synthesis mixtures was close to 9.5. For both procedures the resulting gel mixture was allowed to react at room temperature for 20 h, following which the solid product was obtained by filtration, air dried at room temperature, and finally calcined in air at 650°C for 4 h. The purely siliceous material (designated MMS) was prepared using previously established procedures (7). As reference materials the proton form of MCM-41 (H^+-MCM-41-X, where $X = 20$ is bulk Si/Al ratio) was prepared using the method of Mokaya *et al.* (4), zeolite-HY (Si/Al = 3.65) was from Laporte plc, ultrastable Y zeolite, USY (CBV740, Si/Al = 21) was obtained from PQ Zeolites while amorphous silica-alumina (ASA12, Si/Al = 12) was prepared as described elsewhere (9).

Catalyst Characterisation

Elemental compositions were determined by X-ray fluorescence (XRF). Powder X-ray diffraction (XRD) patterns were recorded using a Philips 1710 powder diffractometer with Cu Kα radiation (40 kV, 40 mA), 0.02° step size and 1-s step time. Textural properties (surface area and pore volume) were determined at −196°C using nitrogen in a conventional volumetric technique by a Micromeritics ASAP 2400 sorptometer. Before measurement each sample was over dried at 280°C and evacuated overnight at 200°C under vacuum. ^{27}Al magic-angle-spinning (MAS) NMR spectra were recorded at 9.4 T using a Chemagnetics CMX-400 spectrometer with zirconia rotors 4 mm in diameter spun at 8 kHz. The spectra were measured at 104.3 MHz with 0.3-s recycle delays and corrected by subtracting the spectrum of the empty MAS rotor. External $Al(H_2O)_6^{3+}$ was used as a reference. To ensure quantitative reliability all calcined samples were fully hydrated and equilibrated with room air prior and to the measurements (10, 11).

Acidity Measurements

The acidity was measured using two methods which employ the "diagnostic" bases cyclohexylamine and pyridine (12, 13). The first method involved thermogravimetric analysis (TGA) of cyclohexylamine containing samples and determines the number of acid sites (principally proton sites) capable of interacting with the base after heat treatment at 250°C. The samples were exposed to liquid cyclohexylamine at room temperature after which they were kept overnight (at room temperature) and then in an oven at 80°C for 2 h so as to allow the base to permeate the samples. The oven temperature was then raised to 250°C and maintained at that temperature for 2 h. The samples were then cooled (under dry nitrogen) to room temperature and their TGA curves obtained using a Polymer Laboratories TG analyser with a heating rate of 20°C/min under nitrogen flow of 25 ml/min. For the mesoporous materials, zeolite HY and ASA12 the weight loss associated with desorption of the base from Brønsted acid sites occurred between 300 and 450°C, with a maxima at ca 370°C. This weight loss was used to quantify the acid content (in mmol of cyclohexylamine per gram of sample) assuming that each mole of cyclohexylamine corresponds to one mole of protons (12, 13). Due to presumably stronger acid sites the maxima for the USY zeolite (CBV740) was higher; for this reason a wider temperature range (280–500°C) was used to calculate the acid content for the USY zeolite. In the second method FTIR spectra of pyridine chemisorbed on the samples were obtained using a Nicolet 205 FTIR spectrometer; 10–15 mg of each sample was pressed (for 2 min at 10 ton/cm^2 pressure under *vacuo*) into a self-supporting wafer 13 mm in diameter. The wafers were calcined under *vacuo* (10^{-3} Torr, 1 Torr = 133.3 N m^{-2}) at 500°C for 2 h, followed by exposure to pyridine vapour at ambient temperature and heating at 100°C for 1 h to allow the pyridine to permeate the samples. The wafers were then allowed to cool to ambient temperature and evacuated for 1 h, following which 1 h thermal treatments in the 100–500°C temperature range were performed and the spectra were recorded at ambient temperature. The difference between the spectra of pyridine adsorbed on the samples at each temperature and that of the reference (activated) was obtained by substraction. The intensities of the resulting spectra (see Fig. 4) were normalised for wafer thickness using lattice vibrations between 1700 and 2000 cm^{-1}.

Catalytic Testing

The conversion of cumene was performed using a tubular stainless steel, continuous flow fixed-bed microreactor (of internal diameter 10 mm) system with helium (25 ml/min) as carrier gas. The catalyst bed (100 mg; 30–60 mesh) was first activated for 1.5 h at 500°C under helium (25 ml/min). For the reaction a stream of cumene vapour in helium was generated using a saturator at room temperature. WHSV of either 5.5 or 4.0 was used. The reaction was first performed at 200°C for 2 h, following which the temperature was raised to 300°C at a rate of 5°C/min and the reaction carried out for a further 2.5 h. The reaction products were separated and analysed using a Carlo Erba HRGC 5300 gas chromatograph on line with the microreactor. Gas chromatographs were obtained automatically on samples of the product stream which were collected at regular intervals using a Valco 6-port valve. The gas chromatographs were used to calculate the percent overall cumene conversion.

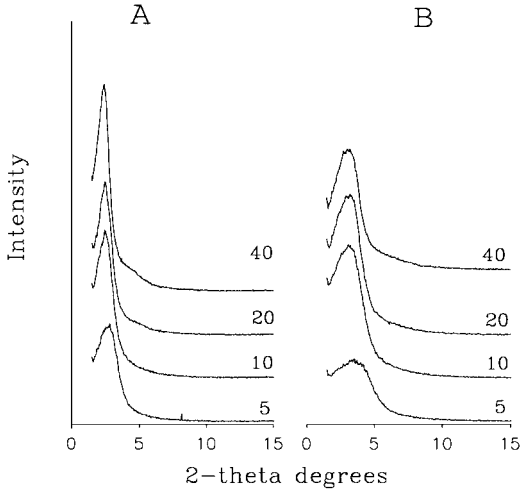

FIG. 1. Powder XRD patterns of calcined Al-MMS samples prepared at the Si/Al ratios shown; (A) with prepolymerisation and (B) without prepolymerisation.

RESULTS AND DISCUSSION

Physical Characterisation

The elemental compositions and textural properties of the materials studied are shown in Table 1. The Si/Al molar ratios of the (calcined) samples are in line with changes in the composition of the gel mixtures indicating that Si and Al are incorporated into the solid framework in proportions largely dependent on the synthesis gel composition. Materials prepared without prepolymerisation have lower amounts of aluminium incorporated. Powder XRD patterns of the calcined samples, which exhibit a single (100) peak, are given in Fig. 1. We note that the XRD patterns obtained here are consistent with those previously reported for similar materials (14–16). Materials prepared with prepolymerisation exhibit a slightly better defined d_{100} peak (with lower FWHM) indicating better hexagonal ordering in these materials, compared to materials prepared without prepolymerisation. The d spacing of the samples (see Table 1) reduces with increasing aluminium incorporation and is lower for materials prepared without prepolymerisation. In both series of samples the decrease in d spacing (as Si/Al ratio decreases) is accompanied with a reduction in intensity and a broadening of the (100) peak suggesting a reduction in the ordering; a similar reduction in hexagonal symmetry has been observed for aluminosilicate MCM-41 molecular sieves (17, 18).

From our observations it is clear that prepolymerisation of the inorganic precursor prior to contact with the template leads to materials with higher amounts of aluminium incorporation and better ordering. This may be related to the ability of the primary amine (dodecylamine) to act both as catalyst for polymerisation of the precursor inorganic species and also as template for subsequent and/or concurrent self assembly of the same. In the case where prepolymerisation is used, the amine acts chiefly as a template while in the absence of prepolymerisation the amine acts both as catalyst for polymerisation and also as template. It appears that this leads to a less efficient formation of a

TABLE 1

Elemental Composition and Textural Properties of Al-MMS Samples

Sample	Si/Al ratio	d_{100} (Å)	Surface area (m^2/g)	Pore volume (cm^3/g)	APD (Å)	a_o (Å)	Wall thickness (Å)
MMS		35	1240	1.68	28.0	40.4	12.4
Al-MMS40	45.6 (62.9)	34 (33)	1200	0.65	25.0	39.3	14.3
Al-MMS20	23.7 (25.9)	33 (31)	1195	0.52	20.0	38.1	18.1
Al-MMS10	13.8 (14.9)	32 (30)	967	0.49	19.8	37.0	17.2
Al-MMS5	6.8 (7.2)	29 (27)	737	0.49	20.5	33.5	13.0

Note. Figures in parenthesis are for samples prepared without prepolymerisation. APD = average pore diameter (determined using BJH analysis). a_o = the lattice parameter, calculated from the XRD data using the formula $a_o = 2d_{100}/\sqrt{3}$.

hexagonal aluminosilicate solid framework. Indeed, using various primary amines (with alkyl length C_8 to C_{16}) we have found that the ability to act as template in the formation of ordered aluminosilicate materials with Si/Al molar ratios similar to the synthetic gel composition increases with alkyl chain length. For example, using octylamine (C_8), we did not obtain hexagonal aluminosilicate materials in the absence of prepolymerisation but we were able to obtain ordered materials via the prepolymerisation method. With C_{10}, C_{12} (which was used for the materials reported here) and C_{14} primary amines it was possible to prepare increasingly well ordered materials in the absence of prepolymerisation with the quality of the materials improving with alkyl chain length of the amine. For hexadecylamine (C_{16}) the effect of prepolymerisation is negligible and both methods yield similar materials. It would thus appear that the "organising" or templating ability of primary amines increases with alkyl chain length.

Further evidence of the incorporation of Al into the solid framework is provided by ^{27}Al MAS NMR spectra of both sets of samples (before and after calcination) shown in Fig. 2. In both cases the spectra of the as-synthesised samples show a sharp resonance from four-coordinate Al at δ 53 indicating that the Al in the synthetic gel mixture is incorporated into the framework. For samples prepared at Si/Al ratio $\leq$10 (Al-MMS5 and Al-MMS10) there is a broad low intensity peak at δ 0 indicating that some of the Al in the samples is extra-framework. It is noteworthy that both series of samples give similar spectra, i.e., neither exhibits higher amounts of extra-framework aluminium. Upon calcination the amount of extra-framework Al increases indicating that in the course of calcination some Al is removed from the framework. Again the spectra for both series of samples are similar indicating that prepolymerisation has no effect on the thermal stability of Al once it is incorporated into the solid framework. This observations suggest that prepolymerisation has no enhancing effect on (crystallographic) ordering at the atomic level and that both methods result in framework walls (in both cases essentially amorphous) which exhibit similar behaviour to thermal treatment. Figure 2 also indicates that the amount of extra-framework Al increases with the proportion of Al in the synthesis gel mixture. However, in accord with MCM-41 aluminosilicates a significant amount of Al is retained in the molecular sieve framework (4, 17, 18). Indeed, the NMR spectra obtained for the calcined Al-MMS samples are similar to those we have previously reported for aluminosilicate H^+-MCM-41 materials (4, 6).

Table 1 also gives the textural parameters of the Al-MMS samples. The elemental analysis and XRD results given above show that Al-MMS materials prepared with prepolymerisation have better hexagonal order than the corresponding materials prepared in the absence of prepolymerisation; for this reason textural parameters were obtained only for materials prepared with prepolymerisation. The surface area, pore volume, and average pore diameter (APD) obtained for the Al-MMS materials are consistent with values previously reported for similar mesoporous materials such as MCM-41 (19, 20). As the amount of aluminium incorporated increases the surface area, pore volume, and average pore diameter (APD) generally decrease. This is probably due to partial collapse of the hexagonal structure during calcination to remove the template and is caused by the instability associated with the presence of increasing amounts of framework aluminium. Figure 3 illustrates the nitrogen sorption isotherms of the samples. The sorption isotherm of the purely siliceous (MMS) material (see Fig. 3, inset) is a typical type IV isotherm similar to that obtained for MCM-41 type materials (19). The hysteresis loop in the 0.35 to 0.6 partial pressure region of the MMS isotherm is indicative of framework mesoporosity while the hysteresis loop at high partial pressure ($p/p_0 > 0.8$) is associated with textural mesoporosity and/or macroporosity (15, 20). The absence of hysteresis in the mesopore filling region in the isotherms of Al-MMS samples is an indication that these material possess pores in the lower mesopore range (20). The reduction in mesopore filling (partial pressure) range as the amount of aluminium incorporated increases suggests a shift of pore size to lower values and is in agreement with the d_{100} spacing and average pore diameters shown in Table 1. It is noteworthy that Al-MMS40 and Al-MMS20 samples with bulk Si/Al molar ratio of 45.6 and 23.7, respectively, do not exhibit any textural mesoporosity and/or macroporosity as evidenced by the absence of hysteresis at high partial pressure (see Fig. 3). Indeed the mesopore volume (PV_m) of these samples (at $p/p_0 \sim 0.5$) were 0.51 cm^3/g for Al-MMS20 and 0.62 cm^3/g for Al-MMS40, i.e., 98 and 95% of the total volume (at $p/p_0 = 0.95$) given in Table 1. However, as the amount of aluminium incorporated increases the development of textural mesoporosity and/or macroporosity occurs for samples Al-MMS10 ($PV_m = 0.43$; 87% of total volume) and Al-MMS5 ($PV_m = 0.39$; 80% of total volume). It is possible that the presence of the hysteresis loop at high partial pressures for Al-MMS10 and Al-MMS5 may be related to macroporous extra-framework alumina generated by partial collapse of the hexagonal framework walls. Considerable amounts of extra-framework alumina in these two samples is suggested by the low intensity broad peak at δ 0 in the ^{27}Al NMR spectra—see Fig. 2.

The wall thickness values, obtained by subtracting the average pore diameter (APD) from the lattice (a_o), given in Table 1 are consistent with those previously reported for similar materials (21). The incorporation of aluminium yields aluminosilicate materials which have thicker walls compared to the purely siliceous sample. If we assume that the incorporation of aluminium into the solid framework is accompanied with an increase in wall thickness, we would

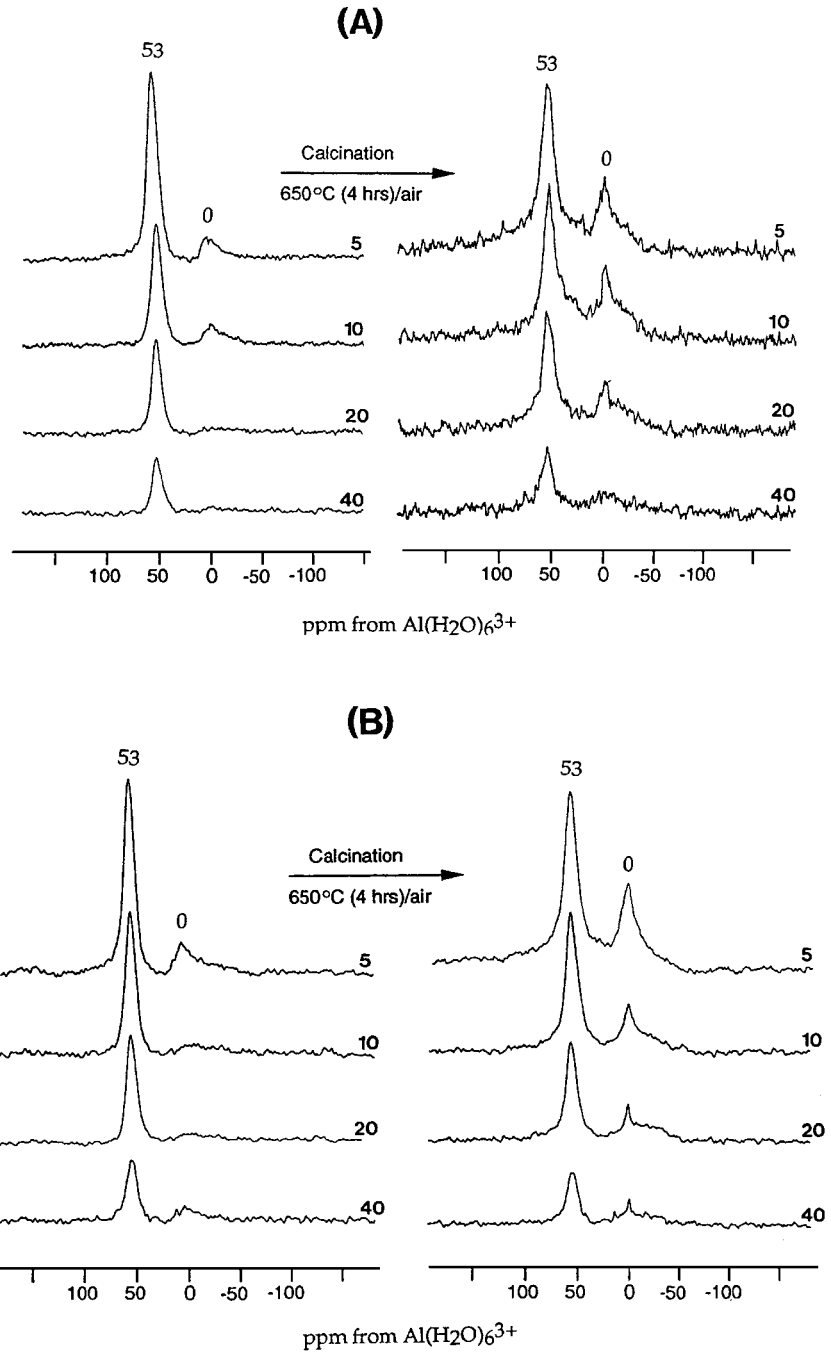

FIG. 2. ^{27}Al MAS NMR spectra of as-synthesised and calcined Al-MMS samples prepared at the Si/Al ratios shown; (A) with prepolymerisation and (B) without prepolymerisation.

expect the wall thickness to increase with decrease in Si/Al ratio. This is true for samples Al-MMS40 and Al-MMS20. However, at lower Si/Al ratios we observed a reduction in the wall thickness with increasing aluminium incorporation which was especially marked for sample Al-MMS5. It is likely that this reduction is due to partial collapse of the framework during calcination as a result of stronger electrostatic interactions between the templating amine and the framework. Indeed we have previously shown that whilst all the amine in the as-synthesised purely siliceous sample is in the neutral form, in the aluminosilicate samples some amine exists in a protonated form and is electrostatically bound to the inorganic framework (7). We have also shown that the amount of protonated amine increases with the amount

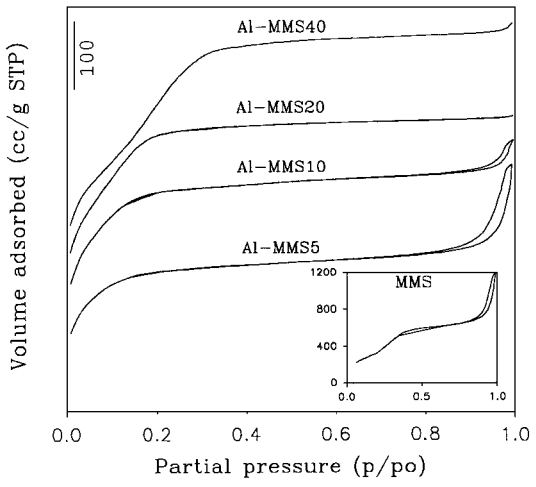

FIG. 3. Nitrogen sorption isotherms of Al-MMS samples. Inset is the sorption isotherm of the purely siliceous (MMS) sample.

of aluminium in the solid framework. It is therefore likely that as the amount of aluminium incorporated increases the attraction between the amine and the framework increases and as a consequence removal of the amine leads to greater local heating and greater collapse of the framework. These observations are consistent with the sorption isotherms shown in Fig. 3; partial collapse of the framework generates textural mesoporosity and/or macroporosity which is observed for Al-MMS10 and to a greater extent for Al-MMS5. We note that the calculation of wall thickness based on XRD and BJH data such as ours is subject to an element of error. We estimate the error in the d_{100} spacing to be 1% and the error in the wall thickness to be ca 3%.

The results discussed above clearly show that the physical (textural) properties of aluminium containing (Al-MMS) materials are similar to those observed for the purely siliceous (MMS) material and equivalent aluminosilicate MCM-41 type materials (21, 22). Furthermore, the powder XRD patterns and ^{27}Al NMR spectra obtained for the calcined Al-MMS materials are similar to those we and others have previously observed for aluminosilicate MCM-41 (4, 6). We have also observed that the Al-MMS materials exhibit considerable thermal stability and are able to maintain an hexagonal structure even after calcination at 900°C for 4 h. This may be related to their thicker walls and greater cross-linking (21). In accord with MCM-41 type materials, the hexagonal ordering in Al-MMS materials is affected by the amount of aluminium incorporated. It is noteworthy that in contrast to a previous report (23) we were able to prepare well-ordered materials with a bulk Si/Al ratio close to 5. Attempts to lower the Si/Al ratio to 2.5 yielded a material with poor ordering, much reduced surface area and pore volume, and a large proportion of extra-framework aluminium.

Characterisation of Acidity

Table 2 gives the acidity values obtained using thermogravimetric analysis (TGA) of Al-MMS samples and the reference materials following adsorption of cyclohexylamine (CHA). The method measures the population of those acid sites which are accessible and sufficiently strong to interact with the base after heat treatment at 250°C and principally determines the proton concentration. In calculating the acidity values we have assumed that each base molecule interacts with one Brønsted acid site (12, 13). We note that, due to the modified method used here, the acid content reported is lower than previously reported by us for the same materials where the samples were not heat treated at 250°C (8). The method reported by us in Ref. (8) determined the total acidity (Brønsted and Lewis) while the modified method used here determines the (medium to strong) Brønsted acid sites which are of interest in catalysis. It is clear from the acidity values that the incorporation of aluminium into the framework generates acid sites which are able to interact with the base. The number of acid sites generated increases as the amount of aluminium in the Al-MMS framework increases. The acidity of Al-MMS samples is generally higher than that of the equivalent protonic aluminosilicate MCM-41 and the amorphous silica-alumina.

Al-MMS materials prepared in the absence of prepolymerisation have lower acidity (20–35% less) compared to corresponding materials prepared with prepolymerisation. This may simply be a reflection of the amount of aluminium incorporated; as discussed earlier prepolymerisation yields materials with greater amounts of aluminium. Ageing of (calcined) samples for a period of 1 year slightly reduces the measured acidity. This may be due to slight dealumination which may occur if the samples come into prolonged contact with moisture; the samples were stored in stoppered vials and no special effort was made to exclude moisture. We note that the retention of acidity, which is an indication

TABLE 2

Acidity of Al-MMS Samples

Sample	mmol CHA/g	
	Fresh samples	Samples aged 1 year
Al-MMS40	0.22 (0.14)	0.20
Al-MMS20	0.36 (0.26)	0.33
Al-MMS10	0.46 (0.36)	0.44
Al-MMS5	0.60 (0.45)	0.56
Zeolite-HY	0.59	
USY	0.17	
ASA12	0.28	
H-MCM-41-20	0.19	

Note. Figures in parenthesis are for samples prepared without prepolymerisation. CHA = cyclohexylamine.

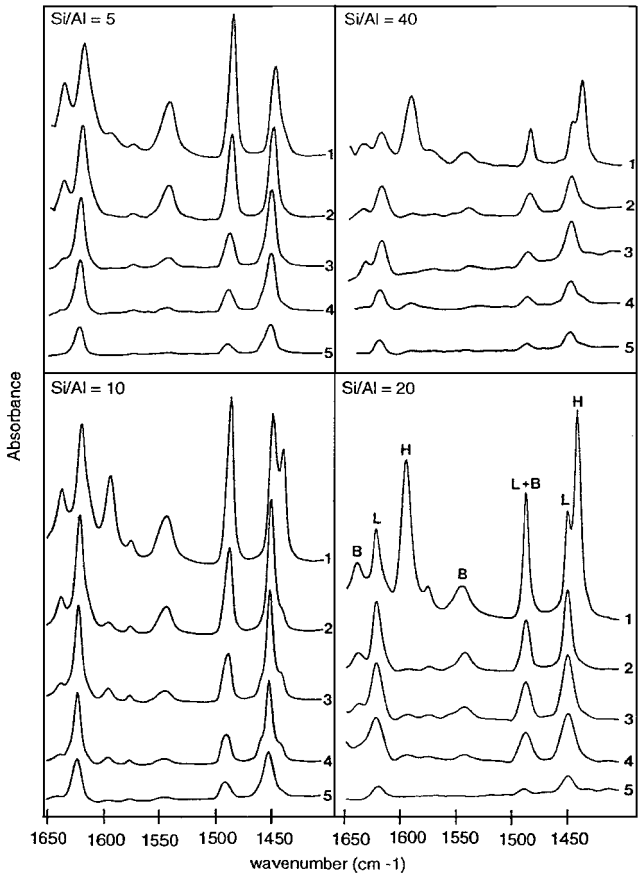

FIG. 4. IR spectra of pyridine on Al-MMS samples prepared at various Si/Al ratio following thermal treatment at (1) 100°C, (2) 200°C, (3) 300°C, (4) 400°C, and (5) 500°C. For peak assignment see spectra for Al-MMS20 (Si/Al = 20). H denotes hydrogen-bonded pyridine; B is Brønsted-bound pyridine; L is Lewis-bound pyridine.

of stability, is remarkable and bodes well for the use of Al-MMS materials as off-the-shelf mesoporous solid acids.

Brønsted and Lewis acidity. To evaluate and analyse the strength and type (Lewis or Brønsted) of acid sites we used the weaker base pyridine. This was done only for samples prepared with prepolymerisation. Figure 4 shows the spectra of pyridine in the region 1650–1400 cm^{-1} following its adsorption on various samples and subsequent thermal treatment at temperatures between 100 and 500°C. All the samples give the expected bands due to hydrogen-bonded pyridine (1447 and 1599 cm^{-1}), Lewis-bound pyridine (1450, 1575, and 1623 cm^{-1}), pyridine bound on Brønsted acid sites (1545 and 1640 cm^{-1}), and a band at 1490 cm^{-1} attributed to pyridine associated with both Lewis and Brønsted acid sites (24). It is interesting to note that, as the Si/Al ratio increases, the relative intensity of the band due to weakly held hydrogen-bonded pyridine increases, when compared to the other diagnostic bands. We have previously observed a similar trend for MCM-41 materials (4). It is likely that hydrogen-bonded pyridine is held on terminal silanol groups. This is consistent with the fact that the concentration of terminal silanol groups per fixed weight of sample is expected to increase with Si/Al ratio and to be greatest for the purely siliceous sample. The infrared spectra of Al-MMS samples clearly shows that the number of both Brønsted and Lewis acid sites increases as the amount of aluminium in the framework increases, thus showing a clear relationship between framework aluminium and the number of acid sites. We believe that the Brønsted acid sites in Al-MMS materials are generated during calcination via decomposition of electrostatically bound dodecylamine template thus generating protons which are retained as charge balancing cations.

The relationship between the amount of framework Al and acidity in Al-MMS samples is much clearer in Table 3 which shows the changes in the number of acid sites (expressed as μmole of pyridine) with evacuation temperature. The number of acid sites was calculated from the IR band areas using the extinction coefficients of Hughes and White (24). It is worth noting that the number of acid sites calculated using pyridine is much lower than that obtained using cyclohexylamine. This is in part due to the lower basicity of pyridine and therefore a tendency to interact only with strong acid sites while cyclohexylamine (a stronger base) interacts with both weak and strong acid sites. It is also possible that the determination of acidity via adsorption of pyridine on wafers obtained by compression is not suited to the tubular morphology of the mesoporous materials; i.e., the compression may damage the pores resulting in diffusional problems and lower accessibility to the acid sites. Table 3 shows that increasing the evacuation temperature reduces the number of acid sites capable of retaining the pyridine. The rate and total reduction in the number of Brønsted acid sites appears greater than that of the Lewis sites. Table 3 clearly indicates that the Brønsted acidity of Al-MMS materials is higher than that of equivalent MCM-41 materials

TABLE 3

Acidity (μmol Pyridine/g Catalyst) of Study Materials Obtained at Various Desorption Temperatures

	(μmol pyridine)/g					
	Brønsted			Lewis		
Sample	200°C	300°C	400°C	200°C	300°C	400°C
Al-MMS40	16	9	2	37	40	27
Al-MMS20	29	13	6	70	73	64
Al-MMS10	36	16	7	88	82	61
Al-MMS5	46	19	9	90	82	67
Zeolite-HY	42	19	4	75	65	54
USY	54	42	18	20	21	22
ASA12	11	6	1.1	53	49	39
H-MCM-41-20	21	7	1.2	42	51	38

and much higher than that of amorphous silica-alumina. Furthermore, the most aluminous sample (Al-MMS5) has total acidity comparable to that of zeolite-HY. Indeed at 400°C, Al-MMS5, Al-MMS10, and Al-MMS20 samples exhibit higher Brønsted acidity compared to zeolite-HY. This indicates that these samples possess a higher proportion of strong Brønsted acid sites compared to zeolite-HY. The number of strong Brønsted acid sites in Al-MMS materials is, however, lower than in USY which as expected possesses the greatest proportion of strong acid sites among the materials analysed. The Lewis acidity of the Al-MMS samples is higher or comparable to that of MCM-41 and zeolite-HY but much higher than that of USY.

The Brønsted/Lewis (B/L) acid site ratios calculated for the Al-MMS samples at each temperature (i.e., 0.41–0.51 at 200°C, 0.18–0.23 at 300°C, and 0.08–0.13 at 400°C) are fairly similar and did not show significant variations with the bulk Si/Al ratio. We believe that this is an indication that the proportion of framework aluminium removed from the Al-MMS framework during calcination does not significantly change with the total amount of framework Al. Our proposal is based on the expectation that if the proportion of extra-framework Al were to increase with increase in aluminium incorporated, we would expect to see a decrease in the B/L ratio as the Si/Al ratio decreases from 40 to 5—assuming that Brønsted acid sites are associated exclusively with framework Al while Lewis acid sites may arise from both framework and extra-framework Al. We note that the B/L ratios for Al-MMS are comparable to those for zeolite-HY (i.e., 0.56, 0.29, and 0.08 at 200, 300, and 400°C, respectively) but contrast with those for the amorphous silica-alumina (0.2, 0.12, and 0.03 at 200, 300, and 400°C, respectively) and those for USY (2.7, 2.0, and 0.82 at 200, 300, and 400°C, respectively). These values suggest that in terms of nature of acidity the Al-MMS samples are closer to HY zeolites than to amorphous silica-alumina but quite different from USY. The B/L ratios for MCM-41 (especially at 300 and 400°C, i.e., ca 0.15 and 0.035, respectively) indicate that the nature of acidity of aluminosilicate MCM-41 is similar to that of amorphous silica-alumina.

The higher Brønsted acidity, despite similar bulk Si/Al ratios in Al-MMS compared to MCM-41 may be related to their mechanism of formation and to the position occupied by 4-coordinate Al in their respective frameworks. Formation of aluminosilicate MCM-41 is dependent on cooperative assembly between the inorganic precursor species (i.e., anionic silicate, aluminosilicate, or aluminate) and the cationic surfactant head groups. It has been suggested that the higher charge density/polarisability of oligomeric silica (compared to aluminosilicate or aluminate anions) favours their binding at the inorganic/organic interface while aluminium containing species occupy the region between silica coated surfactant rods (25). Consequently a large proportion of the Al incorporated in MCM-41 is buried in the inorganic framework and is therefore less efficient at generating *accessible* Brønsted acid sites. On the other hand formation of Al-MMS materials is essentially based on a neutral templating route. The major part of the templating amine are neutral and therefore do not preclude the binding of aluminium containing inorganic precursor at the inorganic/organic interface. We therefore propose that for similar Si/Al ratio, Al-MMS samples have a higher proportion of accessible Al sites compared to MCM-41 and as a result an increased amount of Brønsted acidity. This would suggest that the incorporation of aluminium in Al-MMS materials occurs in such a way as to create actual and accessible cation exchange sites while this may not be the case for MCM-41. Indeed, Weglarski *et al*. have recently reported that the concentration of Brønsted and Lewis acid sites in protonic aluminosilicate MCM-41 is less than the concentration of 4-coordinate aluminium (6). They attributed this to the dehydroxylation of Brønsted acid sites. Although we do not rule out the effect of dehydroxylation, we note that dehydroxylation of itself would not lead to fewer than the expected Lewis acid sites being observed.

Catalytic Evaluation

To study the catalytic activity of Al-MMS samples we have used the conversion of cumene, a reaction which is often used to characterise such aluminosilicate catalysts; 30–60 mesh size catalyst was obtained by pressing the catalysts (for 2 min at 1.5 ton/cm^2 pressure under *vacuo*), followed by crushing and sieving. This procedure was found to have little effect on the textural integrity of the catalysts. Under our reaction conditions the conversion of cumene proceeds almost exclusively via catalytic cracking (on Brønsted acid sites) to yield benzene and propene. Only trace amounts of α-methylstyrene, which may be formed via dehydrogenation over Lewis acid sites, are observed. This indicates that the active sites are Brønsted acid sites; for this reason we shall discuss the catalytic data with reference to Brønsted acidity only. The catalytic evaluation was performed in such a way as to enable a determination of the overall activity, the steady state activity, and the mode of deactivation of the catalysts. The reaction was first carried out at 200°C for 2 h, during which steady state conditions were attained after which the temperature was raised to 300°C, and the reaction carried out for a further 2.5 h. Using this procedure we are able to determine the initial activity at 200°C and the effect of the deactivation, at 200°C, on the reaction at 300°C. It is expected that due to coke formation, the reaction at 200°C will result in blockage of some acid sites thus rendering them unavailable for the subsequent reaction at 300°C. By comparing the "pseudo initial rate" and turnover frequency (TOF) at 300°C with the initial rate and TOF at 200°C we are able to determine the extent to which acid sites are blocked and also whether the blocked acid

TABLE 4

Rate of Cumene Conversion (μmol $g^{-1} \cdot h^{-1}$) and Turnover Frequency, TOF, (h^{-1}) of Study Materials at 200 and 300°C

Sample	200°C		300°C	
	Initial rate	TOF	"Pseudo initial rate"	TOF
Fresh samples				
Al-MMS40	239	1.09	520	2.36
Al-MMS20	453	1.26	804	2.23
Al-MMS10	615	1.34	950	2.07
Al-MMS5	873	1.46	1034	1.72
Aged samples				
Al-MMS40	196	0.98	469	2.35
Al-MMS20	340	1.03	713	2.16
Al-MMS10	480	1.09	873	1.98
Al-MMS5	620	1.11	945	1.69
Reference samples				
Zeolite-HY	610	1.03	673	1.14
USY	1188	7.00	1121	6.59
ASA12	95	0.34	508	1.81
H-MCM-41-20	72	0.38	182	0.96

sites are weak or strong. For this reason and due to the fact that the cracking of cumene is known to require medium to strong Brønsted acid sites, we have used the cyclohexylamine acidity values (which represent a broader range of acid strength) to calculate the TOF. We, however, note that use of Brønsted acidity determined using pyridine at 200°C results in a similar trend in TOF albeit with higher values.

Table 4 gives the initial rate (measured after 2 min time on stream) at 200°C, for the various Al-MMS samples and the reference materials. As expected, for Al-MMS samples the initial rate increases with amount of aluminium. The TOF calculated by dividing the initial rate with the acidity (determined using cyclohexylamine—see Table 2) shows a slight increase with the amount of aluminium. If we assume that the initial rate is a measure of the activity of all the acid sites (since no deactivation and acid site blocking effects are expected), we may then conclude that the activity and proportion of strong acid sites increases with amount of aluminium; i.e., Al-MMS5 has the highest population of strong acid sites and Al-MMS40 has the lowest. This is consistent with the pyridine acidity values shown in Table 3. We note that the samples aged for 1 year have lower initial rates and slightly reduced TOF values. This small reduction in activity is a reflection of the slightly lower acid content of the aged samples occassioned by some dealumination during storage. The reduction in TOF suggests that the dealumination may involve the removal of some strong acid sites but there is no evidence of a weakening of the remaining acid sites. It is therefore clear that the Al-MMS samples are relatively stable to ageing and that after 1 year only a small part of their catalytic activity is lost. Al-MMS samples prepared without prepolymerisation (no data shown) exhibit lower initial rates compared to samples prepared with prepolymerisation but have similar TOF values. This implies the following; (i) at any given (synthetic gel) Si/Al ratio, samples prepared with prepolymerisation have more acid sites (and thus higher cumene conversion rates) than those prepared without prepolymerisation and (ii) the acid strength distribution is the same for both samples, i.e., prepolymerisation increases the number of acid sites but not their strength.

The picture that emerges from the TOF values obtained at 200°C is that the acid strength distribution of Al-MMS samples is only slightly dependent on the Si/Al ratio and that the amount of aluminium mainly affects the number of acid sites but not their strength. The initial rates and TOF values of the reference materials indicate that in general, for the cracking of cumene, Al-MMS samples are more active than zeolite-HY, much more active than amorphous silica-alumina (ASA) and MCM-41 but less active than USY. The order of activity is as follows USY > Al-MMS > zeolite-HY > MCM-41 $\geq$ ASA. This order of activity is consistent with the pyridine acidity values in Table 3 which show that the Al-MMS materials generally have a higher proportion of strong acid sites compared to zeolite-HY, ASA, and MCM-41. We particularly note that catalytic superiority of Al-MMS over equivalent MCM-41 materials; at a bulk Si/Al ratio of 20 (compare Al-MMS20 with H-MCM41-20) the activity of Al-MMS is more than three times greater than that of MCM-41. Since the Al-MMS and MCM-41 materials have similar textural properties we ascribe the difference in catalytic activity to higher acidity in Al-MMS.

The reaction at 300°C probes the activity of acid sites which have not been blocked by coke formation during the reaction at 200°C. As shown in Table 4, in all cases the "pseudo initial rate" at 300°C is higher than the initial rate at 200°C and consequently the TOF values also increase. However, the change in TOF is greater for the less aluminous samples, i.e., the increase is greatest for Al-MMS40 and least for Al-MMS5. As a consequence the trend in TOF values is the reverse of that observed at 200°C, i.e., TOF reduces with increase in amount of aluminium. This observation may be rationalised by considering the effect of deactivation during the reaction at 200°C. It is generally accepted that for any series of materials (with similar textural properties and no significant differences in pore size and structure) catalytic deactivation is a reflection of decrease (via site blocking by coke formation) in available acid sites. It is also true that the strongest acid sites are more prone to blockage by coke formation than weaker sites. Thus the sample with the greatest proportion of strong acid sites tends to be deactivated to the greatest extent. As already mentioned Al-MMS5 has the largest proportion of strong acid sites and therefore a greater proportion of its acid sites are blocked and are unavailable for the reaction

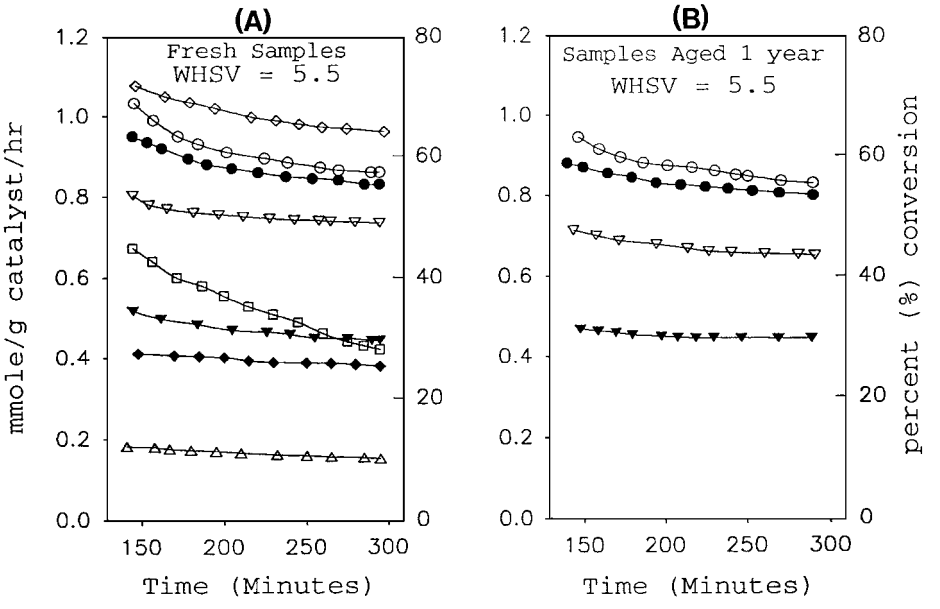

FIG. 5. Deactivation behaviour of fresh and aged Al-MMS samples and reference materials compared at 300°C and WHSV of 5.5. Al-MMS5 (○), Al-MMS10 (●), Al-MMS20 (▽), Al-MMS40 (▼), USY (CBV740) (◇), zeolite-HY (□), amorphous silica-alumina, ASA12 (◆), and H^+-MCM-41-20 (△).

at 300°C. Since progressively fewer sites are blocked as the amount of aluminium reduces, the less aluminous samples retain a greater proportion of their initial acid sites and therefore exhibit a larger increase in TOF due to increase in reaction temperature from 200 to 300°C. Our argument also explains the large increase in TOF observed for ASA and MCM41-20. These samples have a very low proportion of strong acid sites and therefore do not undergo much deactivation during the reaction at 200°C. On the other hand the "pseudo initial rate" and TOF of USY (which contains the highest proportion of strong acid sites among the study materials) is lower than the initial rate and TOF at 200°C. In USY the loss of acidity due to blocked acid sites is high due to the fact that it contains a very large proportion of strong acid sites; this loss of acidity is not compensated for by the increase in reaction temperature.

The curves showing the variation of the rate of cumene cracking (and total conversion) with time on stream at a reaction temperature of 300°C are presented in Figs. 5 and 6. For Al-MMS samples, the rate of deactivation is generally dependent though to a small extent on the Si/Al ratio (see Fig. 5A) and is relatively speaking highest for Al-MMS5 and lowest for Al-MMS40. As the deactivation seems to occur mainly during the first 50 min of the reaction it is likely that the trend observed is due to the strength of acid sites; Al-MMS5 has the largest proportion of strong acid sites and therefore undergoes the most deactivation. Indeed, the amorphous silica-alumina (ASA12) and MCM-41 samples, which mainly possess weak to medium strength acid sites, do not undergo much deactivation. Zeolite-HY on the other hand undergoes considerable deactivation which may be related to pore blocking due to coke formation in the smaller pores. Interestingly the deactivation behaviour of USY is similar to that of the Al-MMS samples. It is clear from our observations that despite having acidity similar to that of zeolite-HY, the Al-MMS samples are generally more active

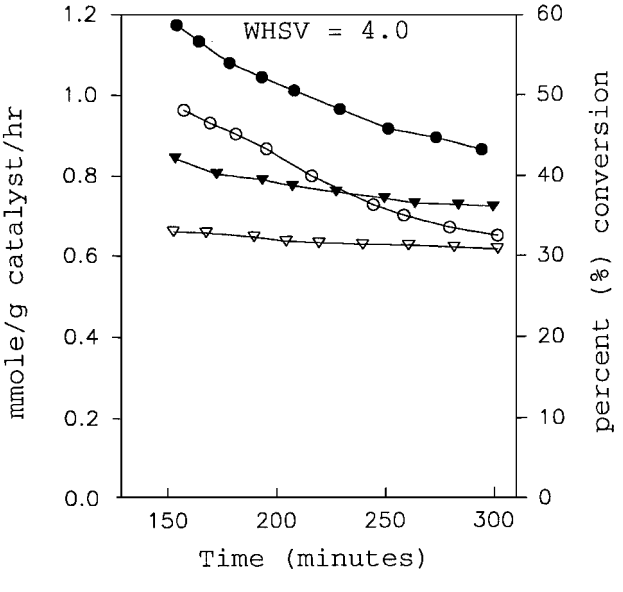

FIG. 6. Effect of prepolymerisation on the deactivation behaviour of Al-MMS samples compared at 300°C and WHSV of 4.0: Al-MMS10 (●, ○); Al-MMS20 (▼, ▽). Filled symbols are for samples prepared with prepolymerisation.

and are more stable to deactivation. Furthermore the rate of deactivation of Al-MMS samples aged for 1 year (see Fig. 5B) is similar to that of fresh samples except that the initial deactivation is less pronounced. This is consistent with the fact that these samples, as discussed earlier, retain most of their acidity. The less pronounced initial deactivation may indicate a small loss of strong acid sites due to ageing. In Fig. 6, using a WHSV of 4.0, we investigate the effect of prepolymerisation on the rate of deactivation of Al-MMS materials (bulk Si/Al 10 and 20). The curves indicate that, due to their higher acidity (see Tables 3 and 4) the activity of samples prepared with prepolymerisation is consistently higher than that of samples prepared without prepolymerisation. However, the rate of deactivation is the same for both series of samples which is consistent with our assertion that they possess sites of similar acid strength distribution.

CONCLUSIONS

We have prepared aluminium containing mesoporous silicas using a primary amine as structure directing agent for the assembly, at room temperature, of aluminosilicate inorganic precursors. The resulting mesoporous materials (designated Al-MMS) have physical and textural properties similar to those previously reported for MCM-41 mesoporous materials but exhibit thicker framework walls and substantially higher Brønsted acidity. Si and Al are incorporated into the mesoporous framework in proportions dependent on the gel Si/Al ratio. The Si/Al ratio affects both the hexagonal ordering and the textural parameters (surface area, pore volume, average pore diameter) which reduce with amount of aluminium incorporated. Calcination of the as-synthesised material removes the occluded amine and generates Brønsted acid sites. The total number of acid sites generated and the proportion of strong acid sites is dependent on the Si/Al ratio. However, the absolute strength of the acid sites is independent of Si/Al ratio. The materials exhibit higher and stronger Brønsted acidity compared to equivalent aluminosilicate MCM-41 or amorphous silica-alumina. Furthermore, the nature of acidity in the Al-MMS materials (as indicated by the Brønsted/Lewis acid site ratio) is closer to that of zeolite-HY than to that of aluminosilicate MCM-41 or amorphous silica-alumina. Their catalytic activity (for the cracking of cumene) whilst lower than that of USY is found to be higher than for equivalent MCM-41 and amorphous silica-alumina and comparable or higher (depending on Si/Al ratio) than that of zeolite-HY. However, the Al-MMS materials exhibit considerable stability to catalytic deactivation which occurs at a lower rate compared to zeolite-HY. Ageing of the materials (for 1 year in the calcined form) has no significant effect on their acidity and catalytic activity. Hexagonal ordering and total Brønsted acidity (but not acid strength) of Al-MMS materials may be improved by using prepolymerised aluminosilicate inorganic precursor.

ACKNOWLEDGMENTS

R.M. is grateful to EPSRC for an Advanced Fellowship and Trinity College, Cambridge for a Research Fellowship. The assistance of Dr. H. Y. He with the NMR measurements and Laporte Adsorbents with surface area determinations is appreciated.

REFERENCES

1. Kresge, C. T., Leonowicz, M. E., Roth, W. J., Vartuli, J. C., and Beck, J. S., *Nature* **359**, 710 (1992).
2. Beck, J. S., Vartuli, J. C., Roth, W. J., Leonowicz, M. E., Kresge, C. T., Schmitt, K. O., Chu, C. T-W., Olson, D. H., Sheppard, E. W., McCullen, S. B., Higgins J. B., and Schlenker, J. L., *J. Am. Chem. Soc.* **114**, 10834 (1992).
3. Huo, Q. S., Margolese, D. I., Ciesla, U., Feng, P. Y., Gier, T. E., Sieger, P., Leon, R., Petroff, P. M., Schuth, F., and Stucky, G. D., *Nature* **368**, 317 (1994).
4. Mokaya, R., Jones, W., Luan, W. Z., Alba, M. D., and Klinowski, J., *Catal. Lett.* **37**, 113 (1996).
5. Sayari, A., *Chem. Materials* **8**, 1840 (1996).
6. Weglarski, J., Datka, J., He, H. Y., and Klinowski, J., *J. Chem. Soc. Faraday Trans.* **92**, 5161 (1996).
7. Mokaya, R., and Jones, W., *Chem. Comm.* **8**, 981 (1996).
8. Mokaya, R., and Jones, W., *Chem. Comm.* **8**, 983 (1996).
9. Anton, O., Wouwe, D. K., Poncelet, G., Jacobs, P., and Martens, J., U.S. Patent 4,720,475 (1988).
10. Ray, R. J., Meyes, B. L., and Marshall, C. L., *Zeolites* **7**, 307 (1987).
11. Man, P. P., Klinowski, J., Trokiner, A., Zanni, H., and Papon, P., *Chem. Phys. Lett.* **151**, 143 (1988).
12. Ballantine, J. A., Purnell, J. H., and Thomas, J. M., *Clay Minerals* **18**, 347 (1983).
13. Breen, C., *Clay Minerals* **26**, 487 (1991).
14. Tanev, P. T., and Pinnavaia, T. J., *Science* **267**, 865 (1995).
15. Tanev, P. T., Chibwe, M., and Pinnavaia, T. J., *Nature* **368**, 321 (1994).
16. Schmidt, R., Akporiaye, D., Stöcker, M., and Ellestad, O. H., "Zeolites and Related Microporous Materials, State of the Art 1994, Studies in Surface Science and Catalysis" (J. Weitkamp, H. G. Karge, H. Pfeifer, and W. Hölderich, Eds.), Vol. 84, p. 61. Elsevier Science, Amsterdam, 1994.
17. Luan, Z. H., Cheng, C. F., Zhou, W. Z., and Klinowski, J., *J. Phys. Chem.* **99**, 1018 (1995).
18. Luan, Z. H., Cheng, C. F., He, H-Y., and Klinowski, J., *J. Phys. Chem.* **99**, 10590 (1995).
19. Branton, P. J., Hall, P. G., Sing, K. S. W., Reichert, H., Scuth, F., and Unger, K. K., *J. Chem. Soc. Faraday Trans.* **90**, 2965 (1994).
20. Rathousky, J., Zukal, A., Franke, O., and Shulzekloff, G., *J. Chem. Soc. Faraday Trans.* **90**, 2821 (1994).
21. Tanev, P. T., and Pinnavaia, T. J., *Chem. Materials* **8**, 2068 (1996).
22. Luan, Z. H., He, H. Y., Zhou, W., Cheng, C. F., and Klinowski, *J. Chem. Soc. Faraday Trans.* **91**, 2955 (1995).
23. Tuel, A., and Gontier, R., *Chem. Materials* **8**, 114 (1996).
24. Hughes, T. R., and White, H. M., *J. Phys. Chem.* **71**, 2192 (1967).
25. Luca, V., MacLaclan, D. J., Bramley, R., and Morgan, K., *J. Phys. Chem.* **100**, 1793 (1996).